

An Open-Source Reproducible Chess Robot for Human-Robot Interaction Research

May 2024

Renchi Zhang, Joost de Winter*, Dimitra Dodou, Harleigh Seyffert, Yke Bauke Eisma

Faculty of Mechanical Engineering, Delft University of Technology, Delft, Netherlands

*Corresponding author: j.c.f.dewinter@tudelft.nl

Abstract

Recent advancements in AI have sped up the evolution of versatile robot designs. Chess provides a standardized environment that allows for the evaluation of the influence of robot behaviors on human behavior. This article presents an open-source chess robot for human-robot interaction (HRI) research, specifically focusing on verbal and non-verbal interactions. OpenChessRobot recognizes chess pieces using computer vision, executes moves, and interacts with the human player using voice and robotic gestures. We detail the software design, provide quantitative evaluations of the robot's efficacy and offer a guide for its reproducibility. The code and datasets are accessible on GitHub: <https://github.com/renchizh/hhh/OpenChessRobot>

Keywords: Artificial Intelligence, Chess, Human-robot Interaction, Open-source, Transfer Learning

1. Introduction

Robots are becoming increasingly common across a variety of traditionally human-controlled domains. Examples range from automated mowers that maintain community lawns to robots in assembly lines and agricultural settings. Recent scientific advancements in AI have enabled new opportunities for intelligent sensing, reasoning, and acting by robots. In particular, the rapid development of large language models, such as ChatGPT, and vision-language models, have lowered the barrier of human-to-robot communication by being able to transform text and images into interpretable actions or vice versa.

As technology advances, it is likely that robots will attain greater capabilities and will be able to tackle tasks previously within the exclusive realm of human expertise. This ongoing evolution may also lead to closer and more productive interactions between humans and robots. At the same time, integrating different AI-based robotic components remains a challenge, and the human-robot interaction (HRI) field lags in terms of endorsing reproducibility principles (Gunes et al., 2022). Encouraging transparent and reproducible research, therefore, remains an ongoing task.

The use of chess as a testbed for evaluating the effect of technology on human perception and behavior traces back to the 18th-century chess automaton Mechanical Turk (Standage, 2002). Furthermore, chess has played an important role in advancing the field of AI, starting with Claude Shannon's chess-playing algorithm (Shannon, 1950) to the success of IBM's Deep Blue (Campbell et al., 2002) and DeepMind's self-play learning algorithm (Silver et al., 2018). In this paper, we incorporate modern AI algorithms into the design of a chess-playing robot to be used for studying HRI. HRI research may benefit from a chess-based setup because the game of chess provides a controlled rule-based environment in which the impact of robots on human players can be precisely measured.

HRI-oriented studies with chess robots have typically employed chess robots to imitate human behaviors and assess the resulting impact on the human opponent. Pereira et al. (2008) and Leite et al. (2013) used the social robot iCat to play chess with children. This robot relies on an electronic chess board as input and emits emotional responses and verbal utterances, guided by an emotion model. Sajó et al. (2011) developed Turk-2, a multimodal chess robot with human-like communication skills, while LC et al. (2021) explored human-robot and robot-robot-human interaction using artistic intervention, where expressive robot arms played chess and embodied distinct personalities.

When an electronic chessboard is not used, a camera is needed to determine if a move has been made and/or what move it was. A common solution is a monocular top-view camera, which has the advantage of not experiencing perspective-induced occlusion, making it relatively easy to identify any changes in the chess position (Golz & Biesenbach, 2015; Kołosowski et al., 2020; Larregay et al., 2018; Luqman & Zaffar, 2016; Srivatsan et al., 2020; Thanh Tra et al., 2018). An exception to this concept is the Gambit chess robot by Matuszek et al. (2011), which does not require a top view but uses a stereo camera instead. This robot was unique because it classified the pieces by type and color, whereas other robots identify and track move-by-move changes from the starting position (e.g., Golz & Biesenbach, 2015; Kołosowski et al., 2020; Larregay et al., 2018; Siraj, 2017).

Other research focuses on the development of computer-vision methods for the detection of the chessboard, and the subsequent classification of the pieces on the chessboard, without always linking these computer-vision methods to a chess robot (Christie et al., 2017; Czyżewski et al., 2020; Ding, 2016; Koray & Sümer, 2016; Ranasinghe et al., 2023; Schwenk & Yuan, 2015; Xie et al., 2018). The detection of the chessboard typically involves line- or edge-detection techniques (Chen & Wang, 2019; Czyżewski et al., 2020; Srivatsan et al., 2020; Wölflein & Arandjelović, 2021; Xie et al., 2018), while the classification of chess pieces commonly uses convolutional neural networks (CNN) (Mallasénn Quintana et al., 2020; Shin et al., 2023; Wölflein & Arandjelović, 2021). Challenges in both cases lie in testing for robustness under various conditions. A common technique to improve classification performance is to verify if the move/position is legal or plausible according to a chess engine. With such methods, it is possible to let the algorithm home in on the most probable classification outcome (e.g., Czyżewski et al., 2020; Mallasénn Quintana et al., 2020; Ranasinghe et al., 2023). Currently, a state-of-the-art method is that of Wölflein and Arandjelović (2021), which used a diverse set of neural network models and achieved a per-square classification accuracy of 99.8%.

Our contribution to the development of the chess robot centers on a software platform that can be reproduced by others by using open-source robotics middleware. The chosen robot arm is widely available in research, while other hardware components can be substituted if required. The OpenChessRobot can detect pieces using computer vision and execute moves. For verbal interaction, we rely on large language models. Specifically, by connecting ChatGPT to the chess engine output, our robot interprets strategies and explains them to humans in natural language. Non-verbally, the robot is able to express its evaluation of the game by either nodding or shaking.

This paper first presents the hardware and software design of the chess robot. It then provides an outline of its core modulus, which include Perception, Analysis & Evaluation, Motion Planning & Execution, and Interaction. Module-specific experiments for performance evaluation are presented as well. The paper concludes with a discussion of the limitations of our robot and future research opportunities in HRI.

2. Hardware and Software Architecture

Our chess-playing robot consists of the following hardware components (Figure 1):

- a Franka Emika Panda robot arm (Franka Emika, 2020) equipped with a Franka Hand and a customized 3D-printed robot gripper. The robot arm has 7 degrees of freedom and is a widely used Collaborative Robot, suited for safe human interaction. It operates on v5.4.0 firmware.
- a ZED2 StereoLabs camera (StereoLabs, 2020).
- a keyboard.
- an external microphone and a speaker, connected to the PC.
- an NVIDIA Jetson Nano (NVIDIA, 2019).
- a Linux PC with Ubuntu 20.04, with a real-time kernel. It is equipped with an Intel I7-8700K processor and an NVIDIA GTX2080 graphics card.

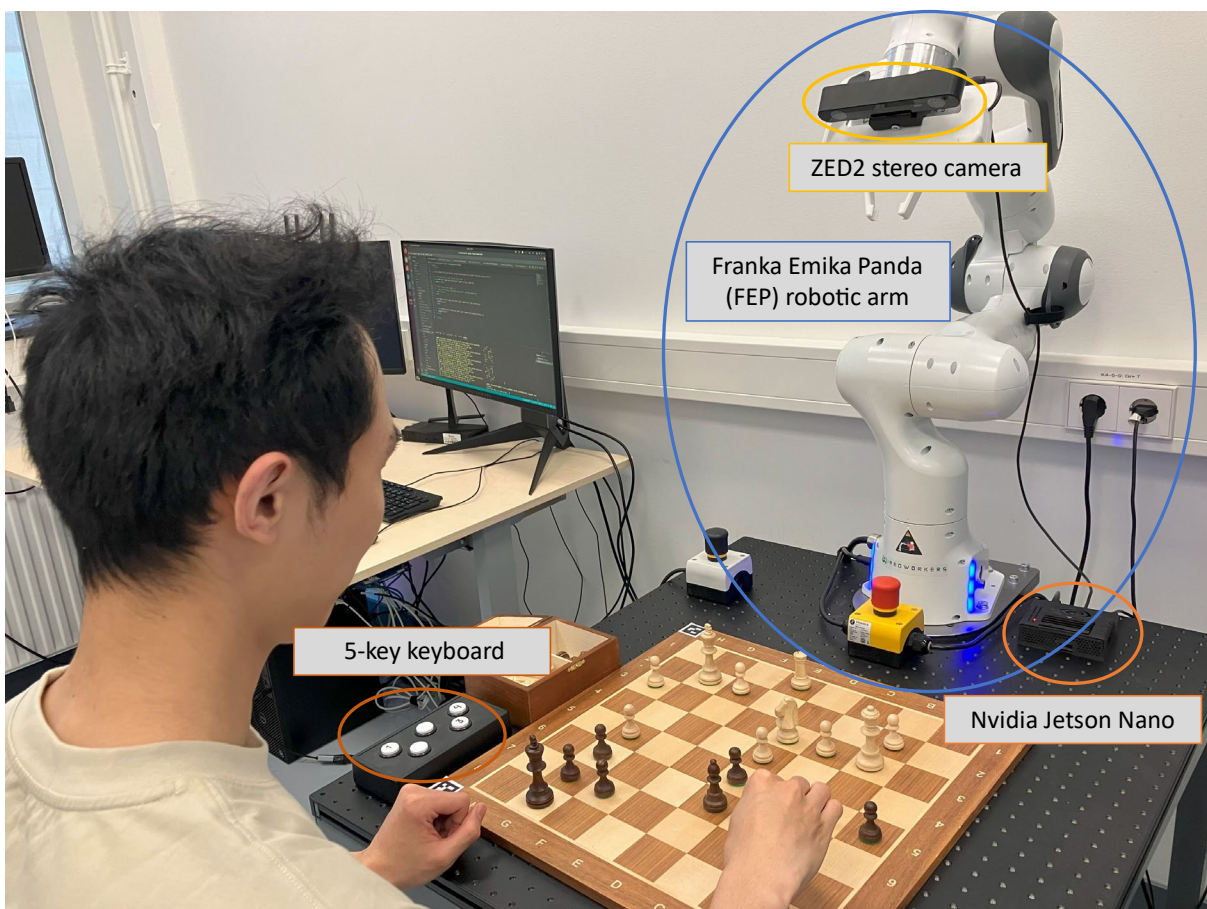


Figure 1. The system at a glance. The whole system consists of a Franka Emika Panda robot arm, a ZED2 stereo camera, and an NVIDIA Jetson Nano computing board.

Our setup includes a number of accessories. These comprise a chessboard (48 × 48 cm), a set of chess pieces (model: Staunton No. 4; ranging in height from 4 to 7.8 cm, and ranging in width from 2 to 4 cm), and four printed ArUco markers. Considering the robot arm's range, the chessboard should be positioned so that the farthest rank remains within 65 cm of the robot. In Figure 1, the distance between the closest edge of the board and the robot is 16 cm.

The robot arm, the Jetson Nano, and the Linux PC connect to a local network via a router. Communication between the arm and the control PC is realized through the Franka Control Interface (Franka Robotics GmbH, 2023) by integrating the Libfranka (0.9.2) library for low-level control and the franka_ros package for the Robot Operating System (ROS) (Quigley et

al., 2009). The ZED2 camera is attached to the Franka Hand via a custom mount, and it interfaces with the NVIDIA Jetson Nano through a USB connection. The Jetson Nano streams the camera view to the PC through ZED SDK v3.5. Considering that our setup uses images from a single camera, the ZED2 camera and Jetson Nano can be substituted with more economical monocular alternatives.

The software architecture of the OpenChessRobot is built upon ROS Noetic (Open Robotics, 2020), which offers common robotics data formats and message-passing among software modules. Figure 2 provides an overview of the software architecture, divided into four modules: Perception, Analysis & Evaluation, Motion Planning & Execution, and Interaction.

The Perception module uses the ZED2 camera SDK to capture the chess game images and relies on a neural-network based chess identifier to translate the game images into text descriptions. The latter identifier requires PyTorch and CUDA runtime. The Analysis & Evaluation module feeds the annotation of the chess game to a chess engine in order to get predicted moves and their corresponding scores. In the Motion Planning & Execution module, the predicted move, accompanied by the 3D chessboard localization results from the Perception module, is used by the MoveIt! motion planner (Coleman et al., 2014) to plan and execute chess moves.

The Interaction module takes the human inputs and manages the OpenChessRobot's verbal and non-verbal feedback. For the verbal feedback, a prompt wrapper, which combines the user request and outputs from the Analysis & Evaluation module, serves as a client of OpenAI's ChatGPT API service and generates the responses to talk with the human.

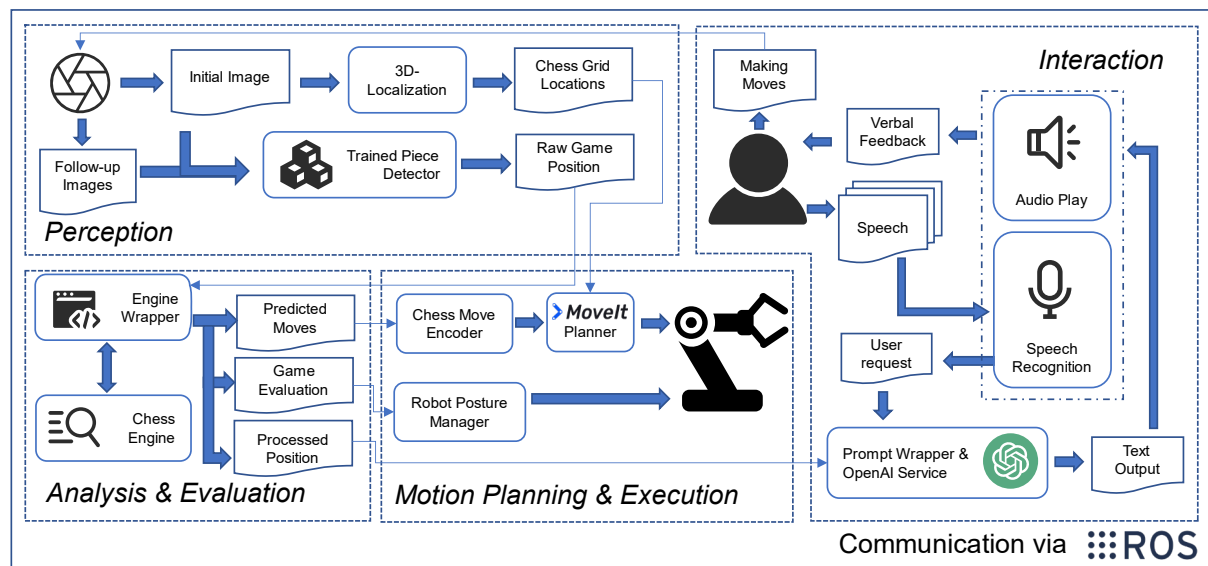


Figure 2. The software architecture of four modules and communications between modules. Within the Perception module, the camera images are used to determine the 3D positions of the squares on the chessboard and identify individual pieces. The identified game position is analyzed through the chess engine wrapper, yielding the best next move and an evaluation of the current board position. The OpenChessRobot then enacts the chess move. Additionally, the robot has the capability to respond through posture and speech.

3. Modules

The Perception module uses computer vision to identify the chessboard and the pieces; it can distinguish between occupied and empty squares and recognize pieces and their color. The perceived game position is sent to the Analysis & Evaluation module, which interfaces with a chess engine to determine the best move. The Perception module also calculates the chess

squares' real-world locations, which are sent to the motion planner for planning the robot's end-effector trajectory to execute chess moves provided by the Analysis & Evaluation module.

The OpenChessRobot runs a data collection pipeline (orange box in Figure 3) and a human-robot gameplay pipeline (yellow box in Figure 3). The data collection pipeline is used to collect real-world data of chess pieces for retraining the Perception module and adapting to a new chessboard. The basic gameplay pipeline allows the robot to play the chess game with a human from any game position.

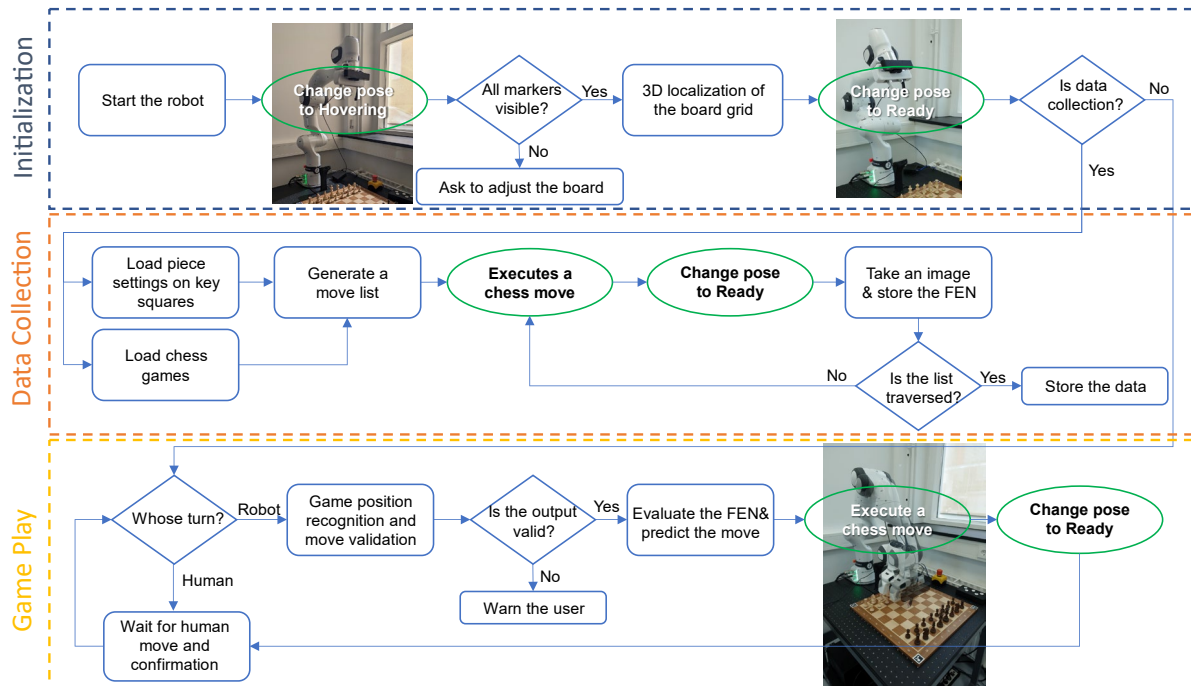


Figure 3. Flow chart of the OpenChessRobot execution using the core modules. The robot uses computer vision to recognize the chessboard and pieces, engages with a chess engine to determine moves, and executes chess moves for gameplay or data gathering. The chart splits into two key workflows: one for collecting data to improve the robot's perception of different chessboards and chess pieces, and another for playing chess with a human.

3.1. Perception

The ability to perceive the chess pieces is a key function of the chess robot. While the commonly used top view resolves the issue of piece occlusion, its practicality is limited because of the limited perspective on the pieces. Adopting lower camera angles and dynamic camera positions to observe the game supports the robot's natural interaction with the human player (see Figure 1). Additionally, our approach relies on RGB images captured by a single camera rather than relying on point clouds (Matuszek et al., 2011), improving the simplicity and reproducibility of our setup.

Figure 4 shows the Perception module of the OpenChessRobot. The module consists of two distinct classifiers, one for occupancy and the other for piece classification.

3.1.1 3D chessboard localization

To manipulate the chess pieces, acquiring their 3D coordinates in the real world is needed. Four ArUco markers are used as indicators of the 3D positions of the chessboard. An image containing these markers, along with the marker length and the camera's intrinsic and extrinsic parameters and distortion coefficients, enables the computation of marker-to-camera translation and rotation using OpenCV.

Training and Inference of the Chess Perception Module

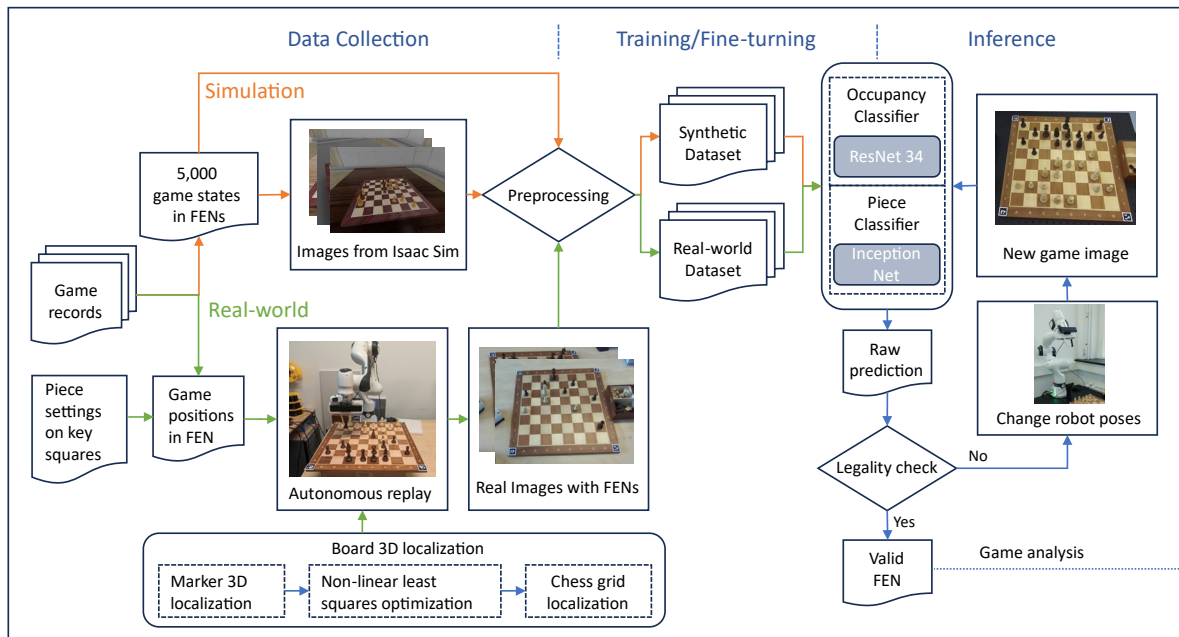


Figure 4. The Perception module of the OpenChessRobot relies on two distinct classifiers, one for occupancy and the other for piece classification. To train these classifiers, we synthesized chess positions in the NVIDIA Isaac Simulator (Makoviychuk et al., 2021) based on previous chess games and assign ground truth labels, including the game positions represented in Forsyth–Edwards Notation (FEN) and pixel coordinates of board corners. In the real-world setup, the robot collects game images from the ready camera pose (Figure 3) after autonomously placing pieces on key squares and replaying given games. These real-world images are then used to fine-tune the classifiers that were initially trained on synthetic datasets.

The board 3D localization is activated when the OpenChessRobot is initialized. The robot moves to a hovering pose to observe the chessboard from above (gray box in Figure 3). Although the robot works with low camera positions most of the time during the game, a vertical camera angle is used for 3D chessboard localization to reduce errors caused by image distortion. Then, a grid is formed for the chess squares using the actual square size and a non-linear least squares algorithm is used to optimize the grid corner positions to be close to the marker positions.

3.1.2 Chess piece detection

In the preceding section, we explained how the 3D coordinates of the squares are estimated. The next task is to identify the chess pieces on each square.

The piece detection model is an extension of a CNN-based model from Wölflein and Arandjelović (2021). We complemented their method by using a different synthetic dataset as well as a real-world dataset to fine-tune the pretrained models in order to effectively handle our real-world chess set.

To synthesize images of chess pieces on a board, we varied backgrounds, lighting conditions, camera poses, and piece locations. A total of 5,000 game positions, randomly selected from games played by grandmaster Bobby Fischer, were used. We synthesized images of selected chess games using the NVIDIA Isaac Simulator (Makoviychuk et al., 2021). Ground truth labels were created, consisting of the game positions represented in Forsyth-Edwards Notation (FEN) and the positions of the board corners. Following a similar approach to previous works (Mallasénn Quintana et al., 2020; Matuszek et al., 2011; Wölflein &

Arandjelović, 2021), the images were cropped into sub-images, each corresponding to a square on the chessboard. Two categories, “empty” or “occupied” were assigned for occupancy classification, while 12 categories (representing the six types of chess pieces in both black and white) were designated for piece classification.

To train the occupancy and piece classifiers with the synthetic data, 80% of the cropped images were used as the training set, while the remaining 20% was evenly split between a test set and a validation set. A ResNet-34 (He et al., 2016) and an InceptionV3 (Szegedy et al., 2015) were trained independently on these two respective training datasets. This is illustrated in the left portion of Figure 4.

To adapt to real world chess, a piece-square dataset was created by manually iterating all the chess pieces on the board. During the iteration, the game positions were recorded in both FEN notation and in images taken at 1080p resolution from the perspective of the robot in the ready pose (Figure 3). A number of training datasets to fine-tune the piece classifier were extracted from the piece-square dataset by using sub-images of chess pieces on key squares. The trained models were evaluated on the remaining portion of the piece-square dataset. Additionally, to evaluate the classifiers’ performance in games, a game dataset was collected by the robot autonomously replaying the provided chess games. Two games played by the grandmaster Michael Adams were used, with the game positions recorded both in FEN and in images, following the same procedure used when collecting the piece-square set. Dataset creation, training settings and evaluation are explained in more detail in the Section 5.1 and Appendix B in the supplementary material.

The preceding chess detection model considered only the position of the chess game. It does not verify the legality of the observed game position and does not possess knowledge of the previous game position. Such information can potentially improve the accuracy of the Perception module. Our legality check consists of two steps: first, it verifies if the game position conflicts with the chess rules, such as detecting no king or too many pawns. If the game position is invalid, it requests a new image—using the same camera pose but with potentially better camera exposure—and reanalyzes it. The robot can also change the camera angle to improve perception. More specifically, in case the predicted game states are detected as illegal, the robot slightly moves to its side in order to capture an image from a different perspective to improve the occupancy and piece classification.

In the second step of the legality check, the robot examines if the recognized chess move is among the legal moves from the prior game position. When the inferred game position and chess move prove to be legitimate, the robot adopts the inference and proceeds with gameplay. If not, the robot will halt its operation and wait for manual correction by the operator.

3.2. Analysis & Evaluation

The processed chess FEN is forwarded to a chess engine wrapper, which uses the Universal Chess Interface (UCI) protocol for interaction with standard engines. Our chess engine wrapper builds upon an existing open-source Python wrapper for Stockfish (Zhelyabuzhsky, 2022). Our system integrates Stockfish 15 (Stockfish, 2022) as the default engine, using a total of 10 CPU threads. The chess engine assigns scores to candidate moves, which are monotonically related to the player’s win rate, should the engine play against an equally strong opponent.

3.3. Motion Planning & Execution

For the planning of the OpenChessRobot’s motions, we rely on the MoveIt! motion planner (Coleman et al., 2014). To determine the joint configurations, an inverse kinematics solver named IKFast is used (MoveIt, 2021). This solver calculates suitable robot joint angles based on the specified end-effector coordinates with respect to the robot’s base.

The robot arm is equipped with a customized gripper (Figure 5), designed to secure the underside of the piece, which is always cylindrical. The gripper is designed to be tolerant to minor deviations between the anticipated pickup positions (square centers) and the actual positions. Consequently, the human (or robotic) chess player is not bound to place a piece exactly at the center of a square.

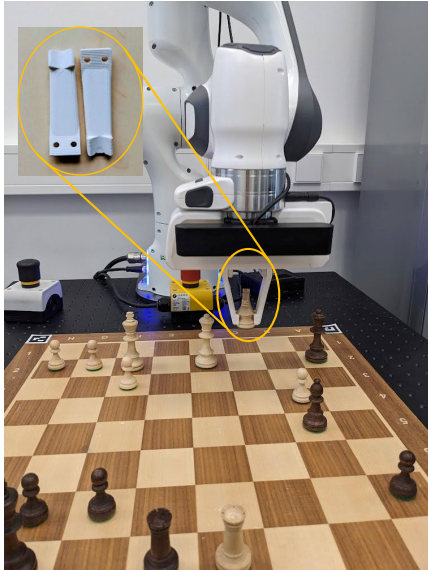


Figure 5. The customized 3D-printed gripper. This gripper has two fingers that can deal with deviations of chess pieces if they are not in the center of a square.

There are two basic robot motions: a sliding motion (Figure 6, left) and a jumping motion (Figure 6, right). If the path between the start and end position of a movement is unobstructed, the robot grasps the piece and pushes it to the destination square. When the path is obstructed, the robot raises the piece to leap over other pieces. Special movements like capture, castling, and en passant are manually programmed as combinations of the two basic motions.



Figure 6. The robot is executing planned trajectories to move chess pieces. Left: The robot slides a pawn from the E2 square to the E4 square. Right: The robot lifts the knight on G1 to jump over other pieces on its way.

A chess move for the robot to execute is provided by the Analysis & Evaluation module in an encoded text format, e.g., g1f310000. The first 4 characters indicate the chess move. Extra information for a move is stored in the remaining characters. Specifically, the fifth to ninth characters stand for whether a move is a jump, capture, castling, en passant, or promotion move.

With the encoded string we create waypoints, using the 3D locations of the start square, the destination square, as well as middle states for special motions. The middle states are generated when the robot needs to lift pieces first rather than slide them on the board. The motion planner receives waypoints and plans the trajectory of the end-effector using Rapidly-exploring Random Trees (RRTConnect; Kuffner & LaValle, 2000), with a 3D box surrounding the chessboard as a workspace constraint. After trajectory planning, velocity/acceleration limits are enforced to the planned trajectory (Kunz & Stilman, 2013).

4. Interactive Modules

As the chess robot aims to be used for human-robot interaction research, providing different modalities for human-robot communication is important. We implemented an interactive gameplay pipeline based on the core modules, as represented in Figure 7. Specifically, based on the human chess performance, the OpenChessRobot can move its head to express its evaluation, and it can verbally express information about move qualities.

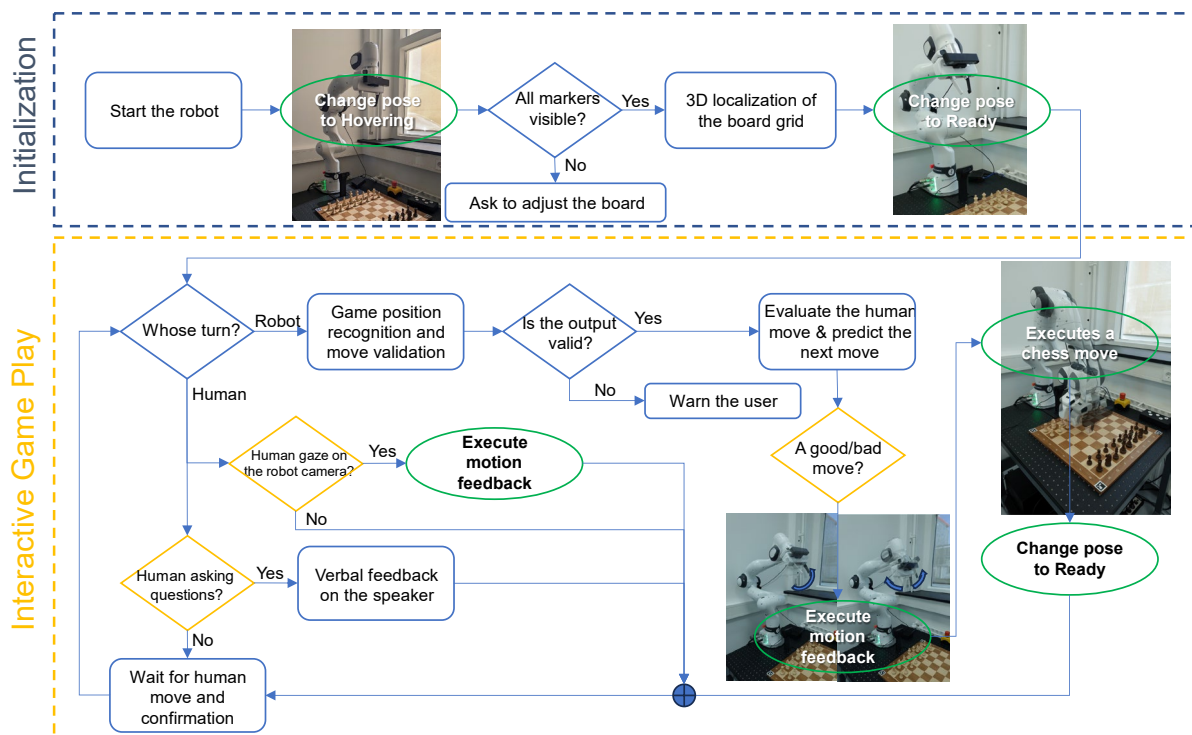


Figure 7. Flow chart of the OpenChessRobot execution using the core modules and Interactive module. As an extension to core modules, the robot has an interactive gameplay pipeline. It evaluates human moves using predefined criteria and provides feedback by adjusting its posture. The system is also programmed to interpret human behaviors, such as gazing or asking questions, to provide a responsive and engaging experience.

4.1. Verbal Interaction

In typical chess games, verbal communication does not hold a central role, although some professional players explained the rationale and inner thoughts of chess moves in “Banter Blitz”. Additionally, chess trainers commonly use verbal feedback to train their students.

OpenAI's ChatGPT has proven to be capable of generating human-like dialogues. However, ChatGPT is unable to properly play chess on its own (Kuo et al., 2023). Our proposed solution relies on combining the analysis from the chess engine with ChatGPT without model fine-tuning.

Depending on the human player's request, the OpenChessRobot can explain the last move or the next move. The process is depicted in Figure 8. Capturing the user's request is achieved through voice recognition. To trigger the voice interaction, the robot should be in the ready pose and waiting for the user's move and before the player has made their move. The player must vocalize specific keywords of "explain the (last) move" or "analyze/predict the (next) move".

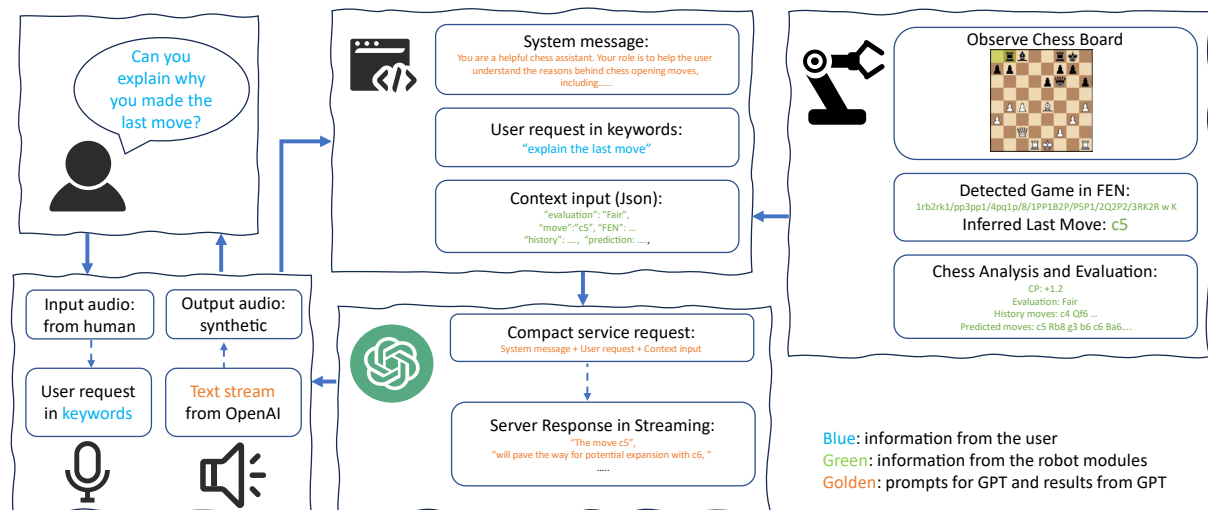


Figure 8. Verbal interaction. In this diagram, the user asks for an explanation of the last move. Then a prompt consisting of a system message, user request, and processed game position is provided to the ChatGPT API to generate the verbal feedback.

When explaining the last move, the move history and the current game FEN are sent to the Analysis & Evaluation module. Alternatively, when the user seeks advice on next moves, the system uses the chess engine to predict several top-ranked moves, along with their game continuations. A wrapper integrates global instructions with the chess game information into a prompt ready for submission to the OpenAI service. The global instructions, which remain the same among different requests, are embedded in a system message (Table 1).

Table 1. Prompt and GPT-4 output to explain the last move (bishop c4)

Prompt:	
System message	You are a helpful chess assistant. Your role is to help the user understand the reasons behind chess opening moves, including their benefits, weaknesses, and overall strategic concepts. There are some instructions on how to respond to the user. Instruction 1: You should always start your response with a short sentence or few words to acknowledge that you've received the user's message and are considering it. Instruction 2: The user prefers concise explanations, so please keep your responses brief. Instruction 3: Your response should be informative and fluid, avoiding bullet points or index numbers. Instruction 4: When analyzing a board, mention one key reason for a move. Try to use the given history moves and predicted future moves. The input will include a user question, a chess FEN for the current game, the move to make, predicted future moves and a move history in a dictionary format under the keys 'question', 'fen', 'move', 'evaluation', 'future' and 'history'. Input:

User message	{'question': 'can you explain?', 'fen': 'r1bqkbnr/pppp1ppp/2n5/4p3/4P3/5N2/PPPP1PPP/RNBQKB1R w KQkq - 23', 'move': 'Bc4', 'evaluation': 'Excellent', \ 'future': 'Bc4 Bc5 d3 Nf6 O-O d6 c3 O-O h3 h6', \ 'history': '1. e4 e5 2. Nf3 Nc6'}
--------------	--

GPT-4-0613:

Sure, I can assist with that. The move Bc4 in this position is known as the Italian Game. The aim of this move is to control the center quickly with your pawn and knight and then put your bishop on its most dangerous square. After this, both white and black usually castle and then start a pawn storm against the opponent's king. In this case, future moves predict a traditional development of pieces with both sides castling kingside. The main goal is to have a solid position and try to exploit tiny advantages.

With the prompt, the OpenAI service is requested to provide an analysis within the specified chess context in a tutor-like tone. To reduce the latency in vocalizing the text responses from the server while maintaining a natural flow in the synthetic voice, the feedback from the server streaming in words/characters is organized in short sentences. A queue for sentences to play sequentially is implemented.

4.2. Non-Verbal Interaction

In human-human communication, non-verbal cues play an important role. In professional chess games, verbal exchanges are often sparse. Apart from the moves played, participants may rely on behavioral cues to understand their opponents.

Posture feedback based on game evaluation

The posture feedback consists of basic nodding and shaking motions executed by the robot's hand (Figure 9). These gestures are triggered based on the chess engine's evaluation. Specifically, the robot enacts nodding or shaking gestures when the reduction in win probability due to the latest move exceeds a predefined threshold.

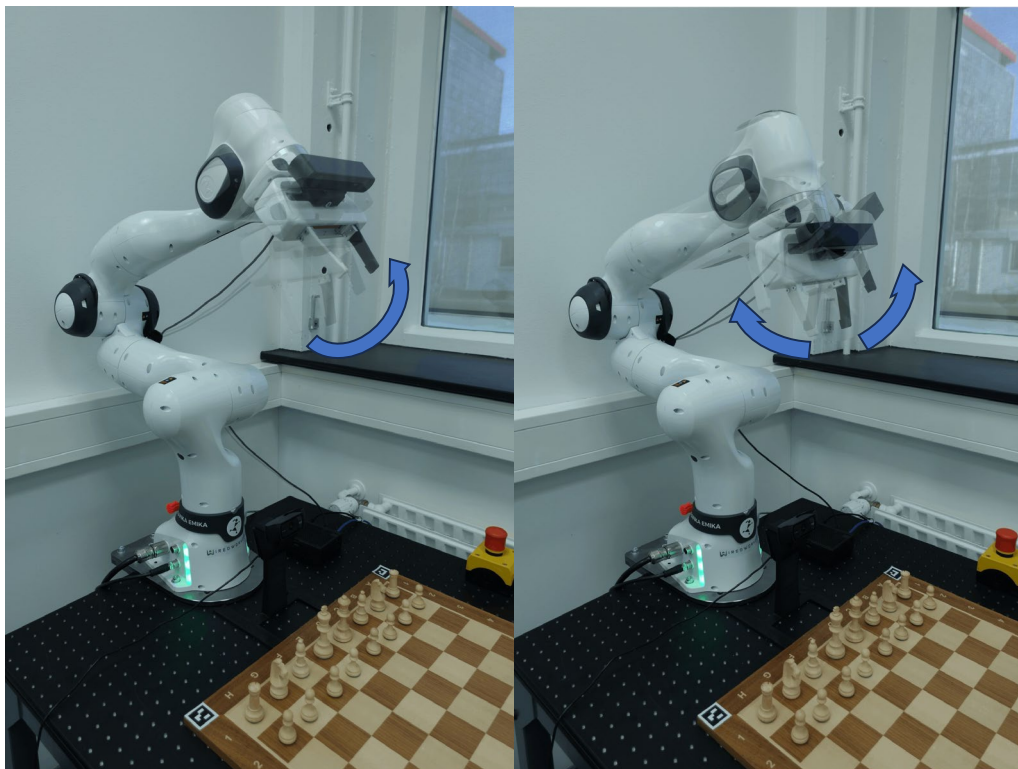


Figure 9. Posture feedback of the robot nodding and shaking head after an evaluated good or bad chess move, respectively.

5. Experimental Evaluation

We performed the following assessments of the chess robot system: (1) Perception module: accuracies of the piece classifiers, (2) Motion Planning & Execution module: grasping a piece across different sections of a square.

5.1. Chess Perception

For the piece classifier of the chess perception module, several training settings were tested, using two sets of key squares, different components of the training dataset, and varying training lengths. The challenge was to identify a training setting that minimizes the number of training samples while achieving good generalization performance.

The two sets of key squares were:

- 3×3 squares, which include intersections between the key files A, E, H and the key ranks 1, 4, 8
- 4×4 squares, which contain intersections between the key files A, E, D, H and the key ranks 1, 4, 5, 8.

The piece-square dataset contains three subsets: default, rotated, and shifted:

- The default dataset (**D**) contains sub-images of 768 unique piece-square pairs (64 squares \times 12 pieces), with each pair occurring once.
- The rotated dataset (**R**) includes sub-images of four types of pieces: white king, white knight, black king and black knight. Kings were rotated twice by 45 degrees (64 squares \times 2 rotations), while knights were rotated four times (64 squares \times 4 rotations) to create different shapes due to their rotational asymmetry (See Figure 10 right). Sixty-four samples of each rotated piece were randomly selected, forming the final rotated dataset.
- The shifted dataset (**S**) contained sub-images with cropping windows shifted in four directions (up, down, left, right). The displacement in each direction was $\frac{1}{4}$ square in length. For each shift direction, all 768 unique piece-square pairs were extracted. The **S** dataset serves as a test set with increased noise.

Additionally, the data recorded by the OpenChessRobot while replaying the games was used as another test set (**G**) to evaluate the piece classifiers trained with piece images on the key squares. Only unique piece-square pairs in each game are extracted, making up the **G** dataset.

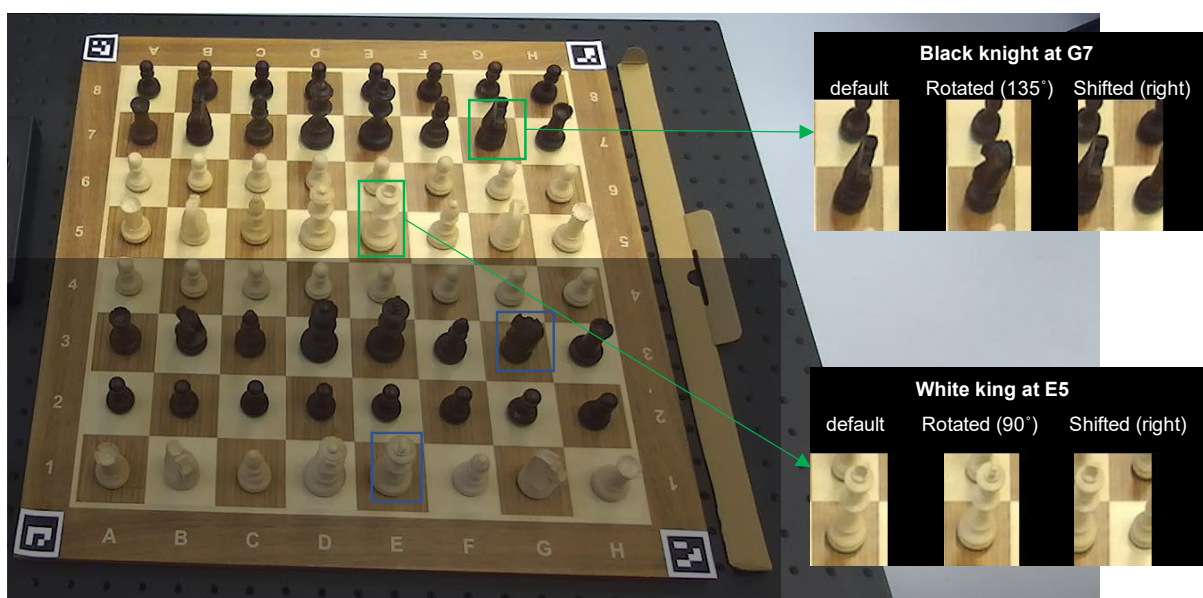


Figure 10. The raw images to create the piece-square dataset. The upper half image is taken without any rotations and the lower half image is taken with 135-degree piece rotations.

Different training and test dataset compositions were extracted from these three datasets.

- The training set (**d**) contained sub-images of each piece on the key squares. The remaining samples in the **D** dataset are divided into a validation set and a test set with a ratio of 20:80.
- The training set (**r**) was generated from the **R** dataset using pieces on the key squares with the 90-degree rotation.
- Similarly, the training set (**rr**) contains all pieces on the key squares with all the rotations from the **R** dataset. The corresponding test sets and validation sets of **r** and **rr** are created in the same manner as the **D** dataset.

The fine-tuning was conducted in two phases: in the first phase, weights of most layers of the model are frozen and only the last layer (head) is trained over epochs with a learning rate of 0.001. In the second phase, all the model's weights are trained with a learning rate of 0.0001. The Adam optimizer is used in both phases.

Following the aforementioned training conditions, the piece classifier models were evaluated on their corresponding test set, as well as on the **S** and **G** datasets. The evaluation results are detailed in Table 2. When comparing the two selections of key squares based on the model accuracies on dataset **G**, it is evident that using 4×4 squares provides more samples for fine-tuning and results in good accuracies with better robustness. Additionally, including the rotated samples in the training set also helps improve performance, but it requires a longer training duration to be effective. Results on the **S** dataset show that using 4×4 squares provides better robustness against the noise caused by piece displacements compared to using 3×3 squares. While longer training durations and adding rotations to the training set yield some improvements, these improvements are not substantial.

Regarding the occupancy classifier, it was found to achieve 100% accuracy on **G** dataset after retraining for 50 epochs using piece sub-images at the 4×4 squares and all the adjacent empty squares.

Table 2. Piece classifier accuracies in different training conditions. The best accuracies on the dataset **S** and **G** are underlined.

Test set	Key squares	3×3									4×4								
		500+500			1000+500			1000+1000			500+500			1000+500			1000+1000		
Training set	Epoch	d	d+r	d+rr	d	d+r	d+rr	d	d+r	d+rr	d	d+r	d+rr	d	d+r	d+rr	d	d+r	d+rr
D-d		0.9924			0.9943			0.9943			0.9978			1.0000			1.0000		
D+R-d-r			0.9794			0.9835			0.9863			0.9939			0.9939				0.9954
D+R-d-rr				0.9915			0.9887			0.9930			0.9984			0.9922			1.0000
S		0.9762	0.9704	0.9684	0.9704	0.9691	0.9759	0.9652	0.9688	0.9740	0.9837	0.9831	0.9844	0.9834	0.9883	<u>0.9886</u>	0.9814	<u>0.9886</u>	0.9844
G		0.9932	<u>1.0000</u>	0.9932	0.9865	0.9662	<u>1.0000</u>	0.9932	0.9865	<u>1.0000</u>	0.9865	<u>1.0000</u>	<u>1.0000</u>	<u>1.0000</u>	<u>1.0000</u>	<u>1.0000</u>	<u>1.0000</u>	<u>1.0000</u>	<u>1.0000</u>

5.2. Grasping of Pieces

An experiment was performed in which the OpenChessRobot was tasked with grasping various pieces positioned on different squares of the chessboard, repeated multiple times. To reduce positional discrepancies, a compensation of 1 cm along the y-axis and 0.55 cm along the x-axis (Figure 11) was applied as the system error.

Specifically, the evaluation focused on testing the grasp performance using the largest piece, the king (4 cm in width, 7.8 cm in height), and the smallest piece, the pawn (2 cm in width, 4 cm in height). These pieces were positioned at each of the four corner squares (A1, A8, H1, H8) and shifted from the edges of the squares to their centers (depicted in Figure 11). Two

shifting distances were used: (1) placing the piece tangent to the square's edge or (2) 0.625 cm away from the edge, corresponding to 1/8 the length of a square. Each piece in each square position was tested 10 times.

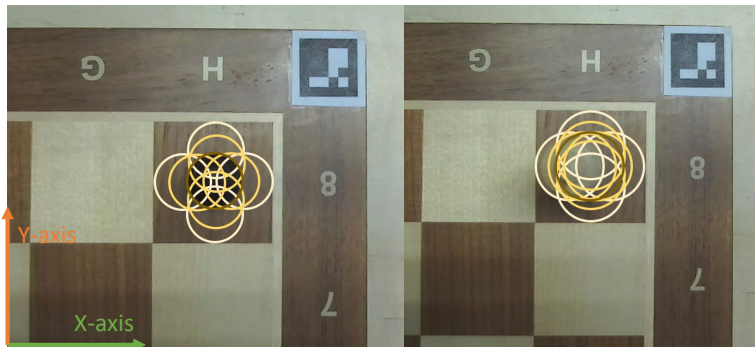


Figure 11. The positions by shifting the piece at square H8. In the left image, the black pawn is in the center without shifting. In the right image, the white king shifts to the left edge of the square. The brown circle shows the center position. The white circles indicate the first shifting distance (to the edge) and the yellow circles indicate the second shifting method (intermediate).

Figure 12 shows the success rates for the different independent variables of the grasping experiment. A distinction is made between three categories: 1) *accurate grasping*: a correct grasp in 10 out of 10 trials, 2) *remedied grasping*: a correct grasp in 8 or 9 out of 10 trials (usually correct grasping occurred here in such a way that the piece slid into the grasper's teeth), and 3) *missed grasping*: a correct grasp in 0 to 7 out of 10 trials. Table 3 shows the corresponding results in numerical form. A trend can be noticed, whereby the grasping was least successful when the piece was positioned toward the edge of the square or towards the 'up' direction, i.e., in the positive direction of the y-axis (see Figure 11), positioned away from the base of the robot arm. It is hypothesized that this effect stems from image projection and coordinate transformation errors in the 3D chessboard localization.

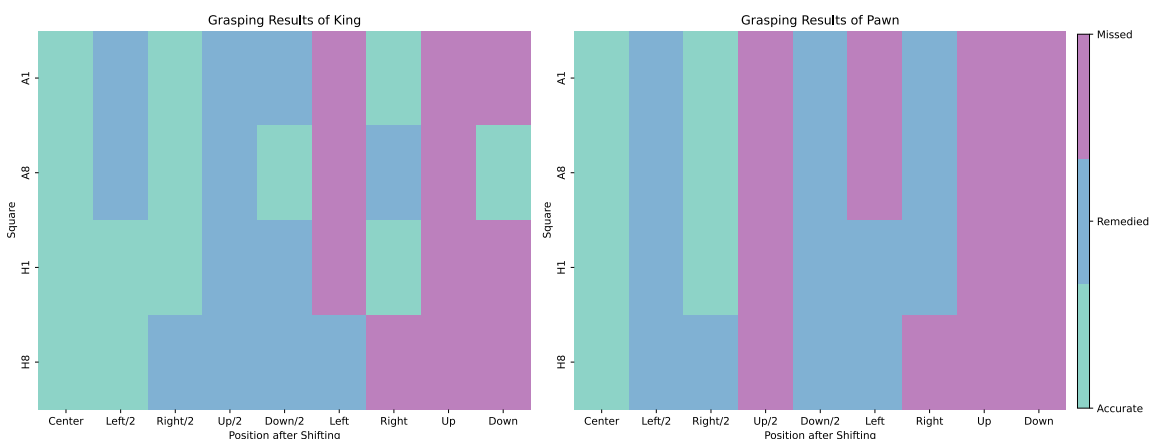


Figure 12. Results from the grasping experiment.

5.3. Human-Robot Chess Play

To assess the core components of the chess robot, a chess game putting a human against the OpenChessRobot was conducted. The robot had control of the white pieces while the human played with the black pieces. To determine its next move, Stockfish 15, with a search depth set to 20, was used.

The OpenChessRobot initiated the game from its ready pose, executed a move, and subsequently returned to its ready pose, awaiting the human player's move. The human player

was prompted to press the middle keyboard button (see Figure 1) upon completing their move. The robot then captured an image, identified the human's move, and made its subsequent move.

Table 3. Piece grasping results. The percentages represent the number of conditions that were marked as 'accurate grasping' or 'remedied grasping'.

Piece	Overall		Shift Distance		Shift Direction			
	Without Shift (n = 4)	With Shift (n = 32)	Halfway (n = 16)	Edge (n = 16)	Left (n = 8)	Right (n = 8)	Up (n = 8)	Down (n = 8)
Pawn	100%	65%	75%	31%	75%	88%	0%	50%
King	100%	78%	100%	31%	63%	88%	50%	63%

To ensure a fair match, the human player also had access to Stockfish 15 to determine their next best move. The game ended when a checkmate was achieved or when the robot and the human repeated a set of specific positions, indicating a tied game. Throughout the experiment, we recorded the time consumption of each robot module as it carried out its respective tasks.

The game ended in a draw after 97 moves. Out of these 97 moves, 7 involved capturing pieces, wherein the robot first removed the captured piece before executing its move; 6 moves required jumping pieces over others, resulting in longer execution times compared to moves made on unobstructed paths. The majority, totaling 83 moves, followed the pick-and-slide approach. The robot executed a castling move twice.

The time taken for the OpenChessRobot to execute its moves is depicted in the left plot of Figure 13. On average, it took 7.33 seconds for the robot to complete a chess move, from its initial position to the resumption of that position after the move. Capture moves, on average, consumed 6.24 seconds. The right plot of Figure 13 shows the time allocation for move detection, evaluation, and prediction. Move detection was typically completed within 1 second, with an outlier attributed to camera failure. Evaluating a single move with Stockfish costs around 1 second. Finding the next move with Stockfish generally consumed approximately 5 seconds, unless the current human move had already been seen when Stockfish searches for the last move. In such cases, the search time was virtually zero, allowing the robot to execute the next move immediately. The relatively large computation time can be explained by the fact that we let Stockfish calculate to a high depth, something that is normally not necessary for amateur-level play.

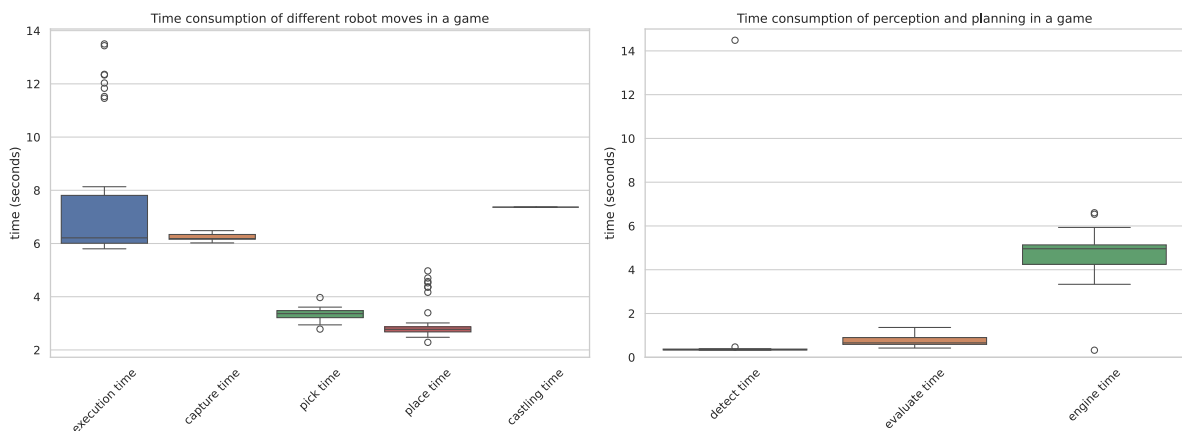


Figure 13. Left: Time consumption of different robot moves in the game. Right: Time consumption of Perception (detect time), Stockfish evaluating a move (evaluate time), and stockfish searching for the next move (engine time).

6. Discussion and Conclusion

In this paper, we introduced an open-source cognitive robot designed for engaging in chess matches with humans. While multiple chess robots have been developed over the years, none have been made available as reproducible platforms, and most of them have not been specifically designed for conducting HRI studies within a chess game context. Our robot takes a unique approach by integrating robust robotic perception, evaluation of gameplay, and move execution. Our development places emphasis on adaptability and reproducibility, rendering it an accessible platform for researchers and enthusiasts alike.

We focused on the game of chess because of its value as a controlled experimental environment where the controllable measurement of both human behavior and machine performance is feasible. Chess also serves as a 'battleground' for Moravec's Paradox, which states that while machines excel at computational tasks (such as playing chess), they traditionally struggle with tasks requiring human-like perception, motor control, and language processing (Moravec, 1988). Our research platform aims to transcend Moravec's Paradox by integrating traditional chess engine capabilities with innovations in human-like perception and the verbalization of moves using synthetic speech. This approach not only challenges Moravec's Paradox but also paves the way for a new line of research. Our platform signals a step toward a new form of robotics that, in essence, revisits the conceptual foundation laid by the Mechanical Turk in the 18th century (Standage, 2002).

Furthermore, the integration of verbal and non-verbal interactions is included to enhance the depth of engagement between humans and the robot. By using a large language model for verbal communication, we have created a solution that bridges this divide between traditional robotic systems and human-like interaction. Future research may include more refined linguistic possibilities by using large language models that are specifically trained or fine-tuned on chess-related text databases (e.g., Feng et al., 2023).

Limitations and future research

Our system has been evaluated across its various modules. The evaluation details validate our design and illuminate possibilities for further research with the system. In terms of interaction methods, our emphasis was on demonstrating the system's capabilities rather than focusing on achieving the state-of-the-art in interactions. The chess engine evaluation is currently only used for posture interactions. Additionally, there is a lack of human-subject experiments that measure user acceptance of the interaction modules.

In the future, we intend to leverage this setup to study how AI-embodied robots influence people during interactions. This will involve the robot communicating with humans through emotional expressions and more natural verbal interactions. Extending the OpenChessRobot's capabilities beyond the chess application to general physical assistance is also an intriguing avenue to explore.

In conclusion, our cognitive chess robot represents a valuable contribution to the field of human-robot interaction, representing a versatile platform for ongoing research. We envision this system not merely as a game companion, but also as a catalyst for scientific research in the area of human-robot interaction.

Funding

This project has received funding from the Cohesion Project of Faculty of Mechanical Engineering, Delft University of Technology.

References

Campbell, M., Hoane, A. J., Jr., & Hsu, F.-h. (2002). Deep Blue. *Artificial Intelligence*, 134, 57–83. [https://doi.org/10.1016/S0004-3702\(01\)00129-1](https://doi.org/10.1016/S0004-3702(01)00129-1)

- Chen, A. T.-Y., & Wang, K. I.-K. (2019). Robust computer vision chess analysis and interaction with a humanoid robot. *Computers*, 8, 14. <https://doi.org/10.3390/computers8010014>
- Christie, D. A., Kusuma, T. M., & Musa, P. (2017). Chess piece movement detection and tracking, a vision system framework for autonomous chess playing robot. *Proceedings of the 2017 Second International Conference on Informatics and Computing*, Jayapura, Indonesia. <https://doi.org/10.1109/IAC.2017.8280621>
- Coleman, D., Sukan, I., Chitta, S., & Correll, N. (2014). *Reducing the barrier to entry of complex robotic software: A MoveIt! case study*. arXiv. <https://doi.org/10.48550/arXiv.1404.3785>
- Czyżewski, M. A., Laskowski, A., & Wasik, S. (2020). Chessboard and chess piece recognition with the support of neural networks. *Foundations of Computing and Decision Sciences*, 45, 257–280. <https://doi.org/10.2478/fcds-2020-0014>
- Ding, J. (2016). *ChessVision: Chess board and piece recognition* (Technical report). Stanford University. https://web.stanford.edu/class/cs231a/prev_projects_2016/CS_231A_Final_Report.pdf
- Franka Emika. (2020). Panda powertool. <https://web.archive.org/web/20200102112015/https://www.franka.de/technology>
- Franka Robotics GmbH. (2023). Franka Control Interface documentation. <https://frankaemika.github.io/docs>
- Feng, X., Luo, Y., Wang, Z., Tang, H., Yang, M., Shao, K., Mguni, D., Du, Y., & Wang, J. (2023). ChessGPT: Bridging policy learning and language modeling. *Advances in Neural Information Processing Systems*, 36. <https://doi.org/10.48550/arXiv.2306.09200>
- Golz, J., & Biesenbach, R. (2015). Implementation of an autonomous chess playing industrial robot. *Proceedings of the 2015 16th International Conference on Research and Education in Mechatronics*, 53–56, Bochum, Germany. <https://doi.org/10.1109/REM.2015.7380373>
- Gunes, H., Broz, F., Crawford, C. S., Rosenthal-von der Pütten, A., Strait, M., & Riek, L. (2022). Reproducibility in human-robot interaction: Furthering the science of HRI. *Current Robotics Reports*, 3, 281–292. <https://doi.org/10.1007/s43154-022-00094-5>
- He, K., Zhang, X., Ren, S., & Sun, J. (2016). Deep residual learning for image recognition. *Proceedings of the 2016 IEEE Conference on Computer Vision and Pattern Recognition*, 770–778, Las Vegas, NV. <https://doi.org/10.1109/CVPR.2016.90>
- Kołosowski, P., Wolniakowski, A., & Miatliuk, K. (2020). Collaborative robot system for playing chess. *Proceedings of the 2020 International Conference Mechatronic Systems and Materials*, Bialystok, Poland. <https://doi.org/10.1109/MSM49833.2020.9202398>
- Koray, C., & Sümer, E. (2016). A computer vision system for chess game tracking. In L. Cehovin, R. Mandeljic, & V. Štruc (Eds.), *Proceedings of the 21st Computer Vision Winter Workshop*, Rimske Toplice, Slovenia.
- Kuffner, J. J., & LaValle, S. M. (2000). RRT-connect: An efficient approach to single-query path planning. *Proceedings 2000 ICRA. Millennium Conference. IEEE International Conference on Robotics and Automation. Symposia Proceedings*, 2, 995–1001, San Francisco, CA. <https://doi.org/10.1109/ROBOT.2000.844730>
- Kunz, T., & Stilman, M. (2013). Time-optimal trajectory generation for path following with bounded acceleration and velocity. In N. Roy, P. Newman, & S. Srinivasa (Eds.), *Robotics: Science and Systems VIII* (pp. 209–216). MIT Press. <https://doi.org/10.7551/mitpress/9816.003.0032>
- Kuo, M. T., Hsueh, C. C., & Tsai, R. T. H. (2023). *Large language models on the chessboard: A study on ChatGPT's formal language comprehension and complex reasoning skills*. arXiv. <https://doi.org/10.48550/arXiv.2308.15118>
- Larregay, G., Pinna, F., Avila, L., & Morán, D. (2018). Design and implementation of a computer vision system for an autonomous chess-playing robot. *Journal of Computer Science & Technology*, 18, e01. <https://doi.org/10.24215/16666038.18.e01>
- LC, R., Benayoun, M., Lindborg, P., Xu, H., Chung Chan, H., Man Yip, K., & Zhang, T. (2021). Power chess: Robot-to-robot nonverbal emotional expression applied to

- competitive play. *Proceedings of the 10th International Conference on Digital and Interactive Arts*, Aveiro, Portugal. <https://doi.org/10.1145/3483529.3483844> .
- Leite, I., Pereira, A., Mascarenhas, S., Martinho, C., Prada, R., & Paiva, A. (2013). The influence of empathy in human–robot relations. *International Journal of Human-Computer Studies*, 71, 250–260. <https://doi.org/10.1016/j.ijhcs.2012.09.005>
- Luqman, H. M., & Zaffar, M. (2016). Chess brain and autonomous chess playing robotic system. *Proceedings of the 2016 International Conference on Autonomous Robot Systems and Competitions*, 211–216, Bragança, Portugal. <https://doi.org/10.1109/ICARSC.2016.27>
- Makoviychuk, V., Wawrzyniak, L., Guo, Y., Lu, M., Storey, K., Macklin, M., Hoeller, D., Rudin, N., Allshire, A., Handa, A., & State, G. (2021). *Isaac Gym: High performance GPU-based physics simulation for robot learning*. arXiv. <https://doi.org/10.48550/arXiv.2108.10470>
- Mallasénn Quintana, D., Del Barrio García, A. A., & Prieto Matías, M. (2020). *LiveChess2FEN: A framework for classifying chess pieces based on CNNs*. arXiv. <https://doi.org/10.48550/arXiv.2012.06858>
- Matuszek, C., Mayton, B., Aimi, R., Deisenroth, M. P., Bo, L., Chu, R., Kung, M., LeGrand, L., Smith, J. R., & Fox, D. (2011). Gambit: An autonomous chess-playing robotic system. *Proceedings of the 2011 IEEE International Conference on Robotics and Automation*, 4291–4297, Shanghai, China. <https://doi.org/10.1109/ICRA.2011.5980528>
- Moravec, H. (1988). *Mind children*. Cambridge, MA: Harvard University Press.
- Movelt. (2021.). IKFast Kinematics Solver. https://docs.ros.org/en/kinetic/api/moveit_tutorials/html/doc/ikfast/ikfast_tutorial.html
- NVIDIA. (2019). NVIDIA Jetson Nano. <https://www.nvidia.com/en-us/autonomous-machines/embedded-systems/jetson-nano>
- Open Robotics. (2020). ROS Noetic installation instructions. <https://wiki.ros.org/noetic/Installation>
- Pereira, A., Martinho, C., Leite, I., & Paiva, A. (2008). iCat, the chess player: The influence of embodiment in the enjoyment of a game. *Proceedings of the 7th International Joint Conference on Autonomous Agents and Multiagent Systems - Volume 3*, 1253–1256, Estoril, Portugal.
- Quigley, M., Conley, K., Gerkey, B., Faust, J., Foote, T., Leibs, J., Berger, E., Wheeler, R., & Ng, A. Y. (2009). ROS: An open-source Robot Operating System. *Proceedings of the ICRA Workshop on Open Source Software*, Kobe, Japan.
- Ranasinghe, P., Ranasinghe, P., & Ashan, V. (2023). ChessEye: An integrated framework for accurate and efficient chessboard reconstruction. *Proceedings of the 2023 Moratuwa Engineering Research Conference*, 177–182, Moratuwa, Sri Lanka. <https://doi.org/10.1109/MERCon60487.2023.10355515>
- Sajó, L., Ruttkay, Z., & Fazekas, A. (2011). Turk-2, a multi-modal chess player. *International Journal of Human-Computer Studies*, 69, 483–495. <https://doi.org/10.1016/j.ijhcs.2011.04.001>
- Schwenk, A., & Yuan, C. (2015). Visual perception and analysis as first steps toward human–robot chess playing. In G. Bebis, R. Boyle, B. Parvin, D. Koracin, I. Pavlidis, R. Feris, T. McGraw, M. Elendt, R. Kopper, E. Ragan, Z. Ye, & G. Weber (Eds.), *Advances in visual computing. 11th International Symposium, ISVC 2015, Las Vegas, NV, USA, December 14–16, 2015, Proceedings, Part II* (pp. 283–292). Cham: Springer. https://doi.org/10.1007/978-3-319-27863-6_26
- Shannon, C. E. (1950). XXII. Programming a computer for playing chess. *The London, Edinburgh, and Dublin Philosophical Magazine and Journal of Science*, 41, 256–275. <https://doi.org/10.1080/14786445008521796>
- Shin, K., Yamsani, S., Mineyev, R., Chen, H., Gandi, N., Lee, Y. J., & Kim, J. (2023). Exploring the capabilities of a general-purpose robotic arm in chess gameplay. *Proceedings of the 2023 IEEE-RAS 22nd International Conference on Humanoid Robots*, Austin, TX. <https://doi.org/10.1109/Humanoids57100.2023.10375209>

- Silver, D., Hubert, T., Schrittwieser, J., Antonoglou, I., Lai, M., Guez, A., Lanctot, M., Sifre, L., Kumaran, D., Graepel, T., Lillicrap, T., Simonyan, K., & Hassabis, D. (2018). A general reinforcement learning algorithm that masters chess, shogi, and Go through self-play. *Science*, 362, 1140–1144. <https://doi.org/10.1126/science.aar6404>
- Siraj, D. S. (2017). JudgeMaster: Automated chess movement validator. *Proceedings of the 2017 National Information Technology Conference*, 112–118, Colombo, Sri Lanka. <https://doi.org/10.1109/NITC.2017.8285662>
- Srivatsan, R., Badrinath, S., & Lakshmi Sutha, G. (2020). Autonomous chess-playing robotic arm using Raspberry Pi. *Proceedings of the 2020 International Conference on System, Computation, Automation and Networking*, Pondicherry, India. <https://doi.org/10.1109/ICSCAN49426.2020.9262351>
- Standage, T. (2002). *The Turk: The life and times of the famous eighteenth-century chess-playing machine*. New York: Walker.
- StereoLabs. (2020). Zed 2. <https://www.stereolabs.com/products/zed-2>
- Stockfish. (2022). Stockfish 15.1. <https://stockfishchess.org>
- Szegedy, C., Vanhoucke, V., Ioffe, S., Shlens, J., & Wojna, Z. (2016). Rethinking the inception architecture for computer vision. *Proceedings of the 2016 IEEE Conference on Computer Vision and Pattern Recognition*, Las Vegas, NV. <https://doi.org/10.1109/CVPR.2016.308>
- Thanh Tra, N. L., Cong, P. T., & Anh, N. D. (2018). Design a chess movement algorithm and detect the movement by images classification using Support Vector Machine classifier. *Proceedings of the 2018 4th International Conference on Green Technology and Sustainable Development*, 335–340, Ho Chi Minh City, Vietnam. <https://doi.org/10.1109/GTSD.2018.8595604>
- Wölflein, G., & Arandjelović, O. (2021). Determining chess game state from an image. *Journal of Imaging*, 7, 94. <https://doi.org/10.3390/jimaging7060094>
- Xie, Y., Tang, G., & Hoff, W. (2018). Chess piece recognition using oriented chamfer matching with a comparison to CNN. *Proceedings of the 2018 IEEE Winter Conference on Applications of Computer Vision*, 2001–2009, Lake Tahoe, NV. <https://doi.org/10.1109/WACV.2018.00221>
- Zhelyabuzhsky, I. (2022). Stockfish. <https://pypi.org/project/stockfish>

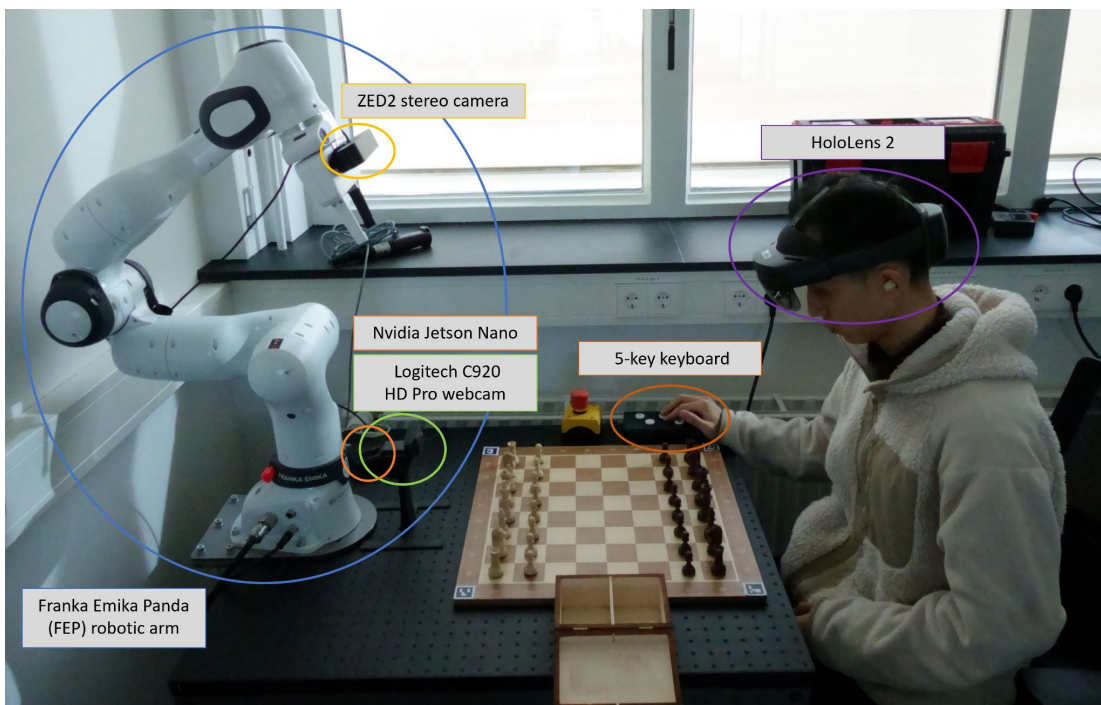
Supplementary Material

Appendix A. Eye gaze tracking with HoloLens 2

In order to monitor the user's eye gaze in real-time, the eye-tracking function of the HoloLens 2 can be used. It is able to determine if the eye gaze vector hits holograms. There are two holograms, namely the Franka robot model and the chessboard model, overlaying on the physical robot and the real chessboard. For this, we implement a digital twin of the robot that follows all the movements of the real robot (see Figure A1). The user's attention distribution can be easily logged by monitoring the gaze-on-hologram status during the interaction.



Figure A1. A digital twin of the chess robot and a model of the chess set in the HoloLens 2. The digital twin and the chessboard in this photo are manually placed next to the physical robot only for the demonstration. In practice, the digital twin and the virtual board are set to be transparent and not visible when the user wears the HoloLens 2.



Appendix B. Dataset creation

A new dataset was collected by placing all the pieces (64 - 1 missing rook) on the board, and then taking photos from the default camera pose. The corresponding labels in FEN format were then created. After row movements, column movements, and rotations, each piece appeared at least once at each square on the board, with rotations. The procedure for creating the dataset is detailed below:

Starting position

The pieces were placed in the middle of the square manually. The camera pose was such that pieces often occluded each other. The adjacent pieces of each piece had both white neighbors and black neighbors.

Image in Dropbox: [Data/piece_square_iteration/raw/img/img_C0_R0_r0.png](#)

Label in

FEN:pppppppp/1nbqkbnr/PPPPPPPP/RNBQKBNR/PPPPPPPP/rnbqkbnr/pppppppp/RNBQKBNR

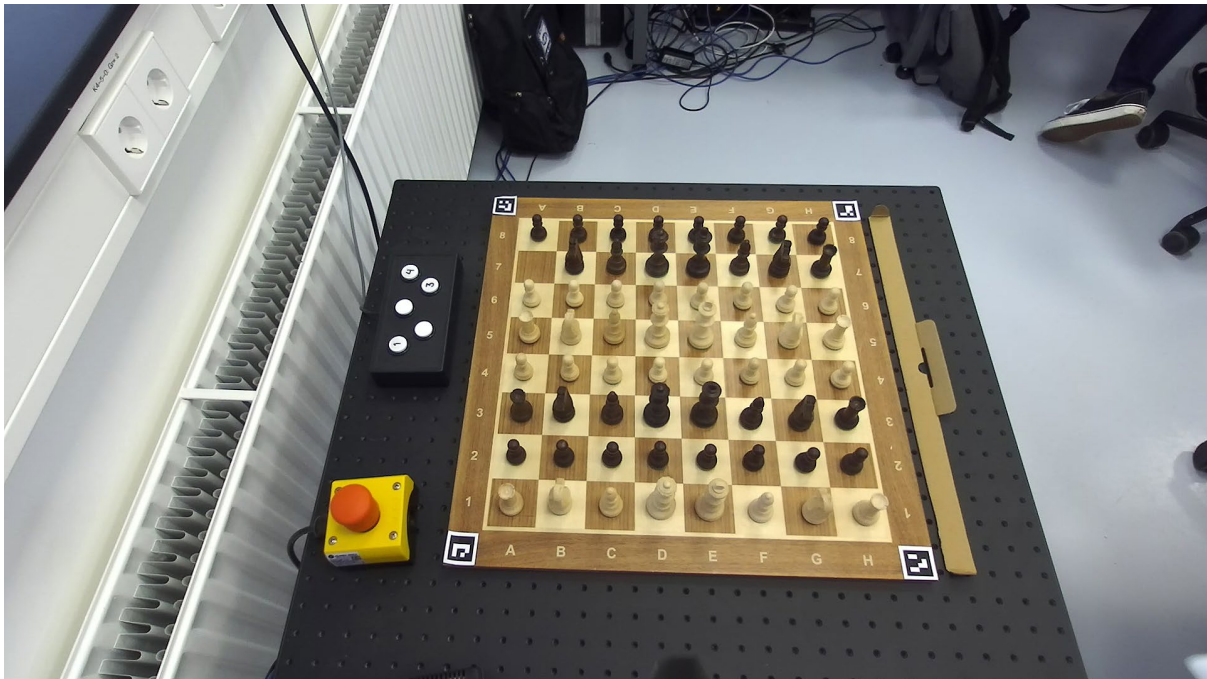


Figure 1. Starting position.

Taking photos of the default and rotated piece positions

At one game position, multiple photos were taken: one photo recorded the default setting. Four additional photos recorded the pieces with rotations. Four types of pieces were rotated because of their rotational asymmetry: white king, white knight, black king, black knight. Kings were rotated twice and knights were rotated four times to create different shapes of the pieces in the image. Each rotation was approximately 45 degrees.

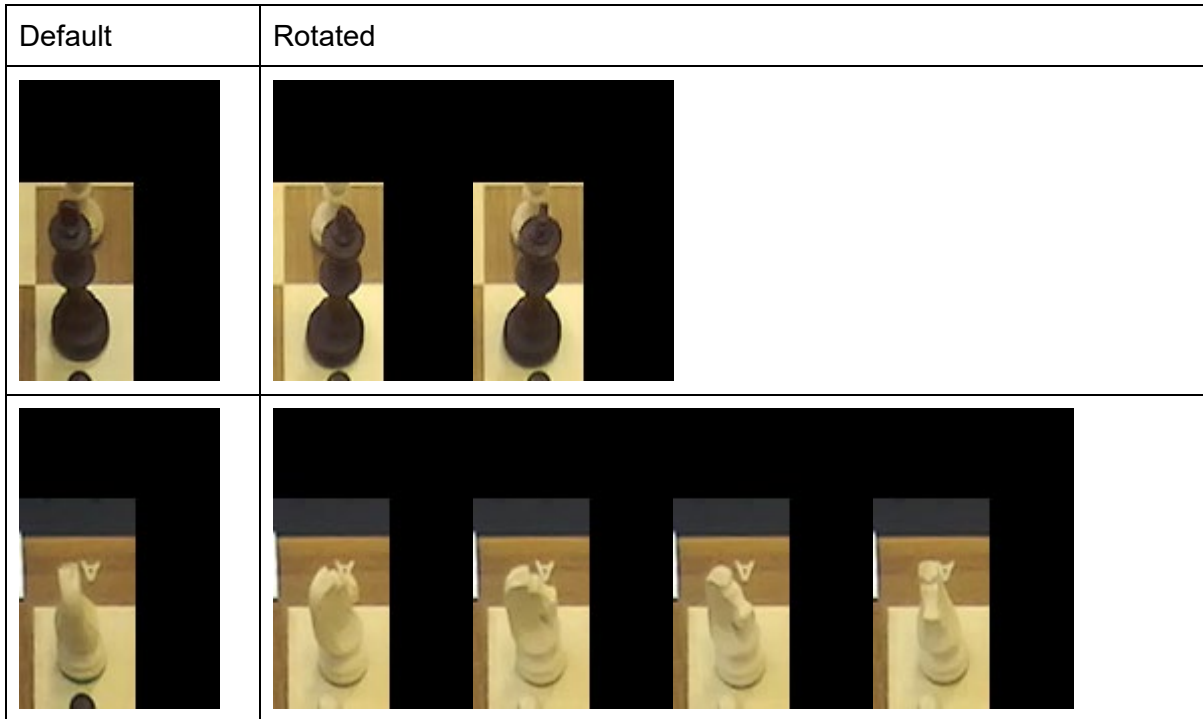


Figure 2. Illustration of piece rotation.

Following the above procedure, at each chess pieces' position, five images were taken (unrotated, both the knight and king rotated twice, knight rotated twice more). Photos are named as: `img_CX_RY_[r0, r1, r2, r3, r4].png`

Shifting the pieces by row

Then, the rows of pieces were moved towards the direction of increasing rank to make a new chess piece position. Then five photos were taken at the new position with the same method mentioned above. The row shifting was repeated 3 times ($R_0 > R_1 > R_2 > R_3$).

Image in Dropbox: `Data/piece_square_iteration/raw/img/img_C0_R1_r0.png`

Label in FEN:

`1nbqkbnr/PPPPPPPP/RNBQKBNR/PPPPPPPP/rnbqkbnr/pppppppp/RNBQKBNR/pppppppp`

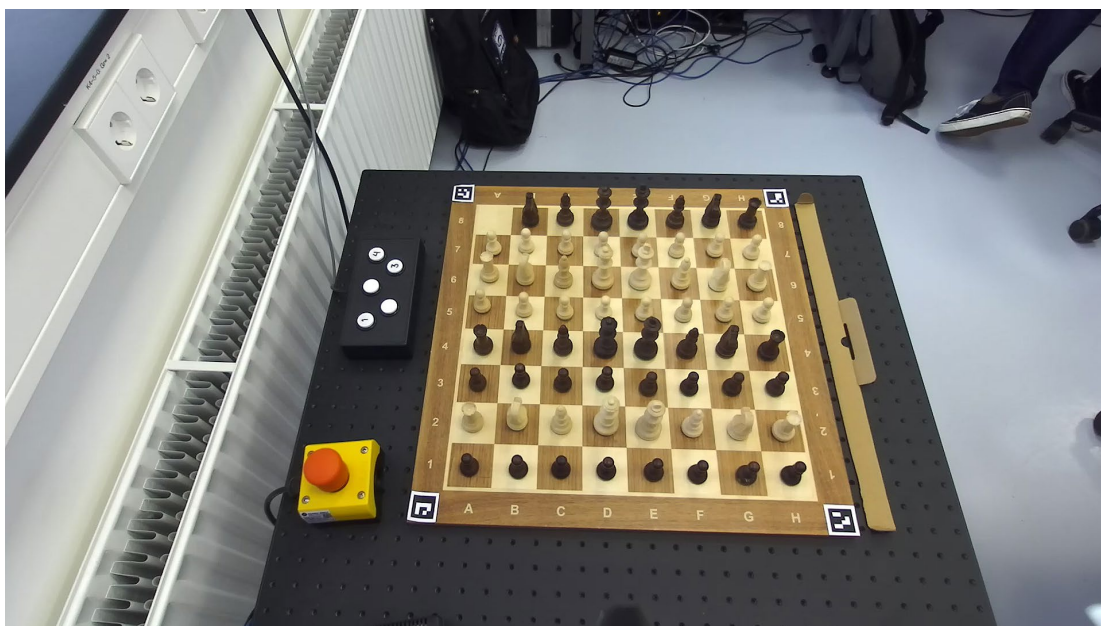


Figure 3. Starting position, after one upward row shift.

Shifting the pieces by column

After shifting the row three times, one additional row shift was realised ($R3 > R0$), in order to recreate the $R0$ game position. After that, a column shift towards the ($A > H$) direction was conducted. ($C0 > C1$), followed by taking photos at this new game position using the same method mentioned above.

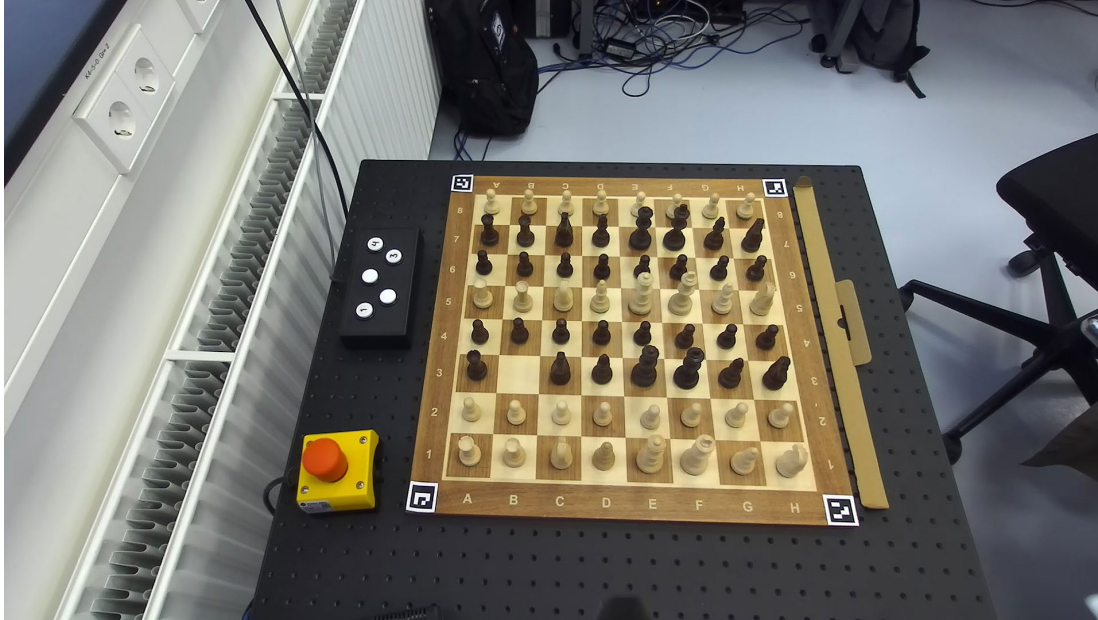


Figure 4. Starting position, after one rightward row shift.

Image in Dropbox: [Data/piece_square_iteration/raw/img/img_C1_R0_r0.png](#)

Label in FEN:

PPPPPPP/rrnbqkbn/pppppppp/RRNBQKBN/pppppppp/r1nbqkbn/PPPPPPP/RRNBQKBN

Creating the datasets

A total of 160 images were collected (4 row movements \times 8 column movements \times 5 rotations) based on which three datasets were created: default, rotated and shifted. Data can be found at: [Dropbox/Renchi Zhang/ChessRobot/Data/piece_square_iteration](#)

The *default dataset* contained 64 sub-images of each unrotated piece. In total there are 64×12 sub-images. For the black and white kings and queens, there is exactly one sub-image per square from the collected images. For the other pieces, the 64 sub-images were randomly selected from the raw dataset for each square.

The *rotated dataset* contained 64 sub-images of each rotated piece (bk, wk, bkn, wkn). Per piece, one of the rotations was picked randomly from the possible rotations for each square.

The *shifted dataset* contained sub-images with their cropping windows shifted into four directions (up, down, left, right). Currently, the displacement in each direction was $\frac{1}{4}$ square in length. For each shift direction, 64×12 sub-images were extracted from the raw image set with the unrotated pieces. The shifted dataset is currently not used in training but only in tests.

Training data selection and train-val-test split

Several squares were selected as key squares for the board. Sub-images of pieces on these squares were used to train the model; this model was then tested on the remaining squares to show its generalization ability. Two sets of key squares were tested:

1. 3×3 :
key_file: A, E, H;

key_rank: 1, 4, 8;
training set: 9 × 12 sub-images;

2. 4×4:
key_file: A, E, D, H;
key_rank: 1, 4, 5, 8;
training set: 16 × 12 sub-images;

The training dataset (**d**) from the default dataset was generated using all sub-images on these key squares.

A training dataset (**r**) was generated from the rotation dataset using all sub-images with 90-degree rotation.

Another training dataset (**rr**) was generated from the rotation dataset using all sub-images with both 90-degree and 180-degree rotations.

Then sub-images of the remaining squares were split into a validation set and a test set using the ratio 20:80. The test sets corresponding to **d**, **r**, **rr** are referred to as **d**, **r**, **rr**.

Before feeding the training set to train the model, some image augmentation was applied on each sub-image randomly. These parameters were set by trial-and-error.

Attributes	Range
brightness/hue/saturation	[-20%,20%]
contrast	[-30%,30%]
scale	[0.8,1.2]
translation	[-0.03, 0.1]

Examples:

